Hindawi
Journal of Nanomaterials
Volume 2021, Article ID 3973784, 8 pages
https://doi.org/10.1155/2021/3973784

Research Article

Drug Release Effect on Large-Clearance TiO_2 Nanotube Arrays Decorated with P25 Nanoparticles

Tao Zhang,[1] **Nannan Liu**,[1] **Yiyuan Zhang**,[1] **and Xiufeng Xiao**[2]

[1]*Department of Orthopedics Institute, Fuzhou Second Hospital Affiliated to Xiamen University, Fuzhou 350007, China*
[2]*Fujian Provincial Key Laboratory of Advanced Materials Oriented Chemical Engineering, College of Chemistry and Materials Science, Fujian Normal University, Fuzhou 350007, China*

Correspondence should be addressed to Tao Zhang; tzhang78@126.com, Yiyuan Zhang; yyzhang2000@126.com, and Xiufeng Xiao; xfxiao@fjnu.edu.cn

Received 19 April 2021; Revised 29 June 2021; Accepted 1 July 2021; Published 22 July 2021

Academic Editor: Hassan Karimi-Maleh

Large-clearance TiO_2 nanotube arrays (LTAs) were synthesized by anodization, and evenly distributed P25 nanoparticles (P25 NPs) decorated on this were prepared by the hydrothermal treatment. The effect of P25 concentrations on the morphology of LATs was studied. LTAs decorated with P25 NPs (LTAs-P25) were loaded with ibuprofen (IBU), and the release properties were investigated. Interestingly, P25 NPs were successfully decorated on the surface of LTAs, with an optimal concentration of 1.2×10^{-3} M. The total amount of drug released from LTAs increased by 49.5% compared to that from TiO_2 nanotube arrays without large clearance. LTAs-P25 provided a lower burst and longer release time.

1. Introduction

Nanotechnology is the science that manipulates matter at molecular and atomic levels. Different application fields of components at the nanoscale level have been explored, such as nanomedicine [1–3] and electrochemical sensor [4–6]. Titania nanotube arrays (TNTs) formed by a self-ordering electrochemical anodization process on Ti have attracted considerable attention due to their biocompatibility, controlled nanotube dimensions, chemical stability, and osseointegration properties. TNTs have been recognized as a promising strategy to develop advanced implants and local drug delivery systems [7, 8]. Previous studies have demonstrated that TNTs as orthopedic implants can promote osteointegration [9, 10]. Moreover, TNTs are used as local drug loading and release systems in the field of bone implants to enhance antibacterial and anti-inflammatory properties, which are desirable for preventing implant-associated infections [11, 12]. However, the nanotube walls are so smooth that the loaded drugs are easily released. The burst release in a short period is not conducive to the sustained release of a drug. Therefore, the surface modification of TNTs is an important means to improve the drug loading capacity of this kind of biomedical material and realize the sustained and controlled release mode [13].

P25 nanoparticles have a diameter of about 21 nm and a large specific surface area and are composed of 80% anatase titanium dioxide and 20% rutile titanium dioxide. P25 is widely used in biomedicine and has attracted much attention because of its high antibacterial activity, biocompatibility, and low toxicity or no toxicity in vitro and in vivo [14, 15]. In this paper, we synthesized the large-clearance TiO_2 nanotube arrays (LTAs) by anodizing Ti foils. The obtained LTAs have a large average pore diameter and big void spaces among the tubes. Then, we decorated P25 on the surface of LTAs to prepare a drug delivery system via the hydrothermal method and loaded it with ibuprofen (IBU) by the vacuum drying method. The large void spaces and pore diameter of LTAs facilitated the intercalation of the decorating and loading IBU into the nanotubes. The increased roughness and surface area of LTAs improved the adsorption capacity of the nanotube to achieve sustained release of the drugs. It

would be reasonable to believe that the LTAs-P25 will become promising candidates for drug delivery.

2. Experimental Details

2.1. Preparation of LTAs. The LTAs were obtained through a typical anodization approach, in which a two-electrode anodization setup was made. Ti was used as a working electrode, and a platinum sheet was used as a cathode; the two electrodes were separated by a distance of 10 mm. First, titanium foils were mechanically polished to achieve a mirrorlike finish and then ultrasonically cleaned in acetone for 15 min, followed by chemical etching for 10 s in nitric acid/hydrofluoric acid (HNO_3/HF), rinsed with deionized water, and air-dried. The prepared Ti foil sample was then immersed in a lactic acid electrolyte and 10 vol% DMSO containing 0.35 wt% NH_4F, first under a voltage of 55 for approximately 15 min, followed by 50 V for 24 h at 30°C. After anodization, the LTAs were rinsed with deionized water and dried at room temperature.

2.2. LTAs Decorated with P25 (LTAs-P25). P25 nanoparticles were loaded on LTAs by the hydrothermal method. LTAs-P25 is prepared by the following steps: firstly, P25 nanoparticles with different concentrations are added into distilled water and then uniformly stirred for 15 min after ultrasonic treatment. The solution and LTAs were placed in a hydrothermal kettle for heat treatment (85°C, 12 h). After cooling and washing, annealing treatment followed (5°C/min, 400°C, 2 h).

2.3. Drug Loading and Releasing on LTAs-P25. The loading of IBU was realized by the vacuum drying method. A certain amount of IBU/ethanol was absorbed and spread on the LTA surface, put in a vacuum drying oven, and treated at 18°C for 2 h, and the step was repeated five times. LTAs-P25 loaded with IBU was placed in PBS, and a drug release experiment was carried out at 37°C for 15 days. A 500 μL sample was sucked regularly, and then, the same volume of blank PBS was added to measure the drug release by ultraviolet-visible spectroscopy at 264 nm, and a drug release curve was drawn to judge drug release performance.

2.4. Characterization. Field emission scanning electron microscopy (FE-SEM, JSM-7500F) was used to analyze the surface morphology of the samples. Philips X'Pert MPD using Cu K radiation generated at 40 kV and 30 mA was used to characterize the crystalline phases of the samples. The amount of IBU released into the PBS at 264 nm was detected by UV-vis spectroscopy (TU1900). The detection of sample vibrations was measured on Nicolet Avatar 360 FTIR.

3. Results and Discussion

3.1. The Morphology and XRD Analysis of LTAs and LTAs-P25. Figures 1(a)–1(d) show the SEM images of the morphology of the prepared LTAs before (Figures 1(a) and 1(b)) and after (Figures 1(c) and 1(d)) decoration with P25 NPs. Specifically, Figure 1(a) is the top view SEM image with a low magnification, with the inset as its cross-section before decoration with P25. Figure 1(b) shows the image with a high magnification before decoration with P25. Figures 1(a) and 1(b) clearly show that the LTAs not only exhibit perfect morphologic characterization (such as self-organized, highly ordered, and free-standing) but also show the optimized geometrical architectures, the large void spaces, large pore diameters of ~320 nm, long tube lengths of ~3.3 μm, and large intertubular spaces of 100-150 nm. This suggests that the special structure of the LTAs provides both the highly facilitated entrance for P25 nanoparticles and very easy growth points for homogenous modification [16]. Compared with conventional TiO_2 nanotube arrays prepared in the glycerol/H_2O system, the LTAs have shown an increase of almost 110 nm in diameter and a significantly shorter length. Figures 1(c) and 1(d) present the morphologies of the as-prepared LTAs-P25. It indicates that P25 NPs are successfully decorated on the surface of TNTs, with the pore diameter decreasing to 100 ± 10 nm after decoration (Figure 1(c)). The previous study has shown that the prepared nanotube has a relatively smooth tube wall when the organic electrolyte is involved in the anodic oxidation process [17]. In contrast, the specific surface area and roughness of the nanotubes were increased after the P25 nanoparticles are loaded on LTAs by a hydrothermal method.

Figure 2 shows the XRD patterns of LTAs (Figure 2(a)), pure P25 (Figure 2(b)), and LTAs-P25 (Figure 2(c)). Notably, all the samples exhibited the characteristic diffraction peaks of anatase TiO_2 at $2\theta = 25.3^\circ$ (JCPDS Card No. 21-1272) [18]. This may be due to the transformation of the TNT phase from amorphous to anatase phase after annealing treatment of LTAs at 400, and then, the characteristic peak of anatase TiO_2 appeared. As shown in Figure 2(b), compared to pure P25, the diffraction peak observed at $2\theta =$ 27.4, 36.1 was attributed to the characteristic diffraction peak of rutile-type TiO_2 (JCPDS Card No. 21-1276) [19]. Although it has been found by SEM that P25 was successfully modified to LTAs, a diffraction peak attributed to rutile-type TiO_2 did not appear. Only about 20% of rutile titanium dioxide is present in P25. These results indicate that very little rutile TiO_2 was successfully modified to LTAs, resulting in P25 providing a less intense diffraction peak of rutile TiO_2 not observed [20].

3.2. The Impact of Different Concentrations of Decoration Solution. Figure 3 shows the microtopography of LTAs prepared by the hydrothermal method at different P25 concentrations (7.5×10^{-4}, 1.2×10^{-3}, and 1.6×10^{-3} M) at 85°C for 12 h. The results showed that the amount of P25 loaded on the nanotube surface was positively correlated with the concentration of P25 solution, and only the optimal batch of 1.2×10^{-3} M resulted in the uniform decoration of P25 on the LTAs (Figure 3(b)). Figure 3(a) shows that only a small quantity of P25 NPs coated the LTAs, with no noticeable decrease in diameters because the P25 solution concentration was negligible (7.5×10^{-4} M). In contrast, a significant amount of P25 NPs coated the pores and void spaces of nanotubes when a high concentration of P25 solution was used (1.6×10^{-3} M), leading to occlusion of most of the nanotubes, as shown in Figure 3(c). The solution

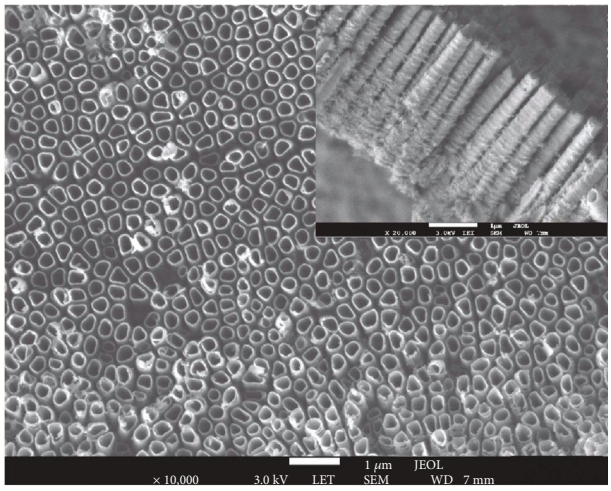

(a)

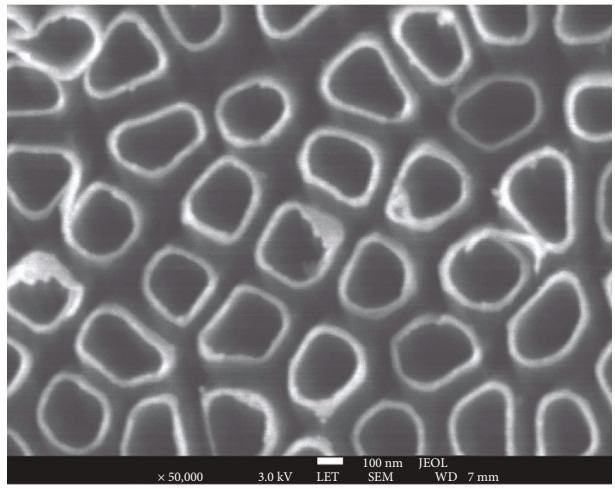

(b)

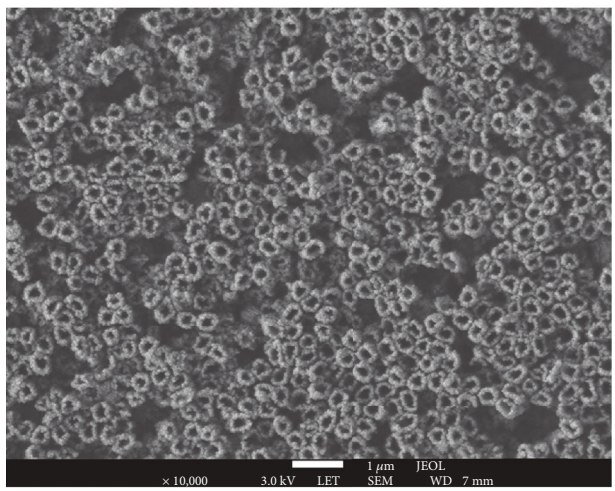

(c)

Figure 1: Continued.

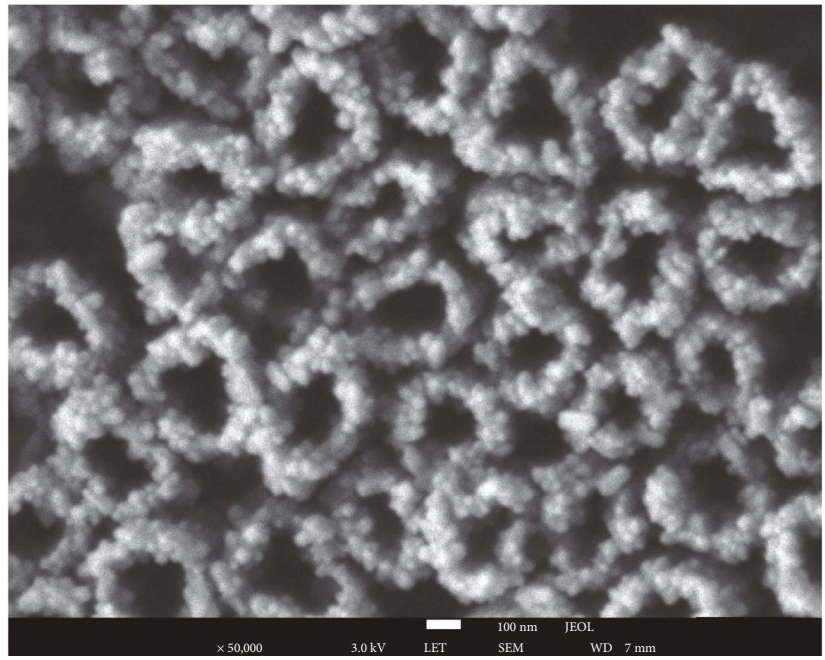

(d)

Figure 1: SEM images of TiO_2 nanotube arrays: (a) top view before decorated P25; (b) high magnification before decorated P25; (c) top view after decorated P25; (d) high magnification after decorated P25.

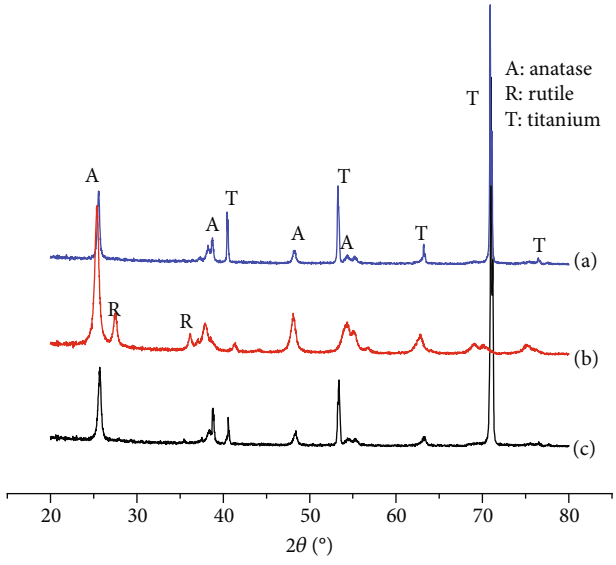

Figure 2: XRD patterns of two samples: (a) LTAs; (b) pure P25 particle; (c) LTAs-P25.

concentration is at a high level, resulting in a large amount of P25 deposited in the nozzle and gap of LTAs, which is not conducive to a large amount of drug loading. Therefore, excessive P25 NPs sintered and agglomerated after heating. Obviously, the loading capacity and effect of Figure 3(b) are better than those of Figures 3(a) and 3(c), and it is a sample with the best morphology and larger surface area. It can be judged that the optimum concentration for loading P25 in LTAs more uniformly is 1.2×10^{-3} M (Figure 3(b)).

3.3. The Morphology of the Samples after Drug Loading. Figures 4(a) and 4(b) present the SEM images of the morphology of the prepared LTAs and LTAs-P25 after IBU loading, indicating that the drug was successfully loaded onto TiO_2 nanotube arrays by the vacuum drying method. A significant amount of the drug is clustered, and most nanotubes are entirely covered (Figure 4(a)). In contrast, Figure 4(b) shows that IBU distributed on the pores homogeneously, and void spaces of LTAs-P25 are entirely covered by IBU.

Furthermore, Figure 4(b) illustrates that IBU is adsorbed on the surface and is incorporated partly into the nanotubes, indicating that the increased specific surface area and roughness of LTAs after hydrothermal treatment are conducive to drug dispersion and absorption.

3.4. XRD Analysis of the Samples after Drug Loading. Figure 5 shows the XRD pattern of the drug-loaded samples. Compared with the XRD pattern of pure IBU, the characteristic diffraction peak credit belongs to IBU-loaded LTAs and LTAs-P25 appeared at $2\theta = 6.08$, 12.21, 16.70, and 20.19 (JCPDS card number 32-1723), respectively. The successful loading of the drug on the two samples is confirmed by the vacuum drying method. Compared with Figure 5(b), a stronger characteristic peak of IBU appears in Figure 5(a), which indicates that the modified sample has stronger adsorption capacity, so that a large amount of IBU is effectively loaded on LTAs-P25.

3.5. In Vitro Release of IBU. Figure 6 presents comparative drug release curves of ibuprofen loaded into LTAs and LTAs-P25. It indicated that the release of IBU from LTAs

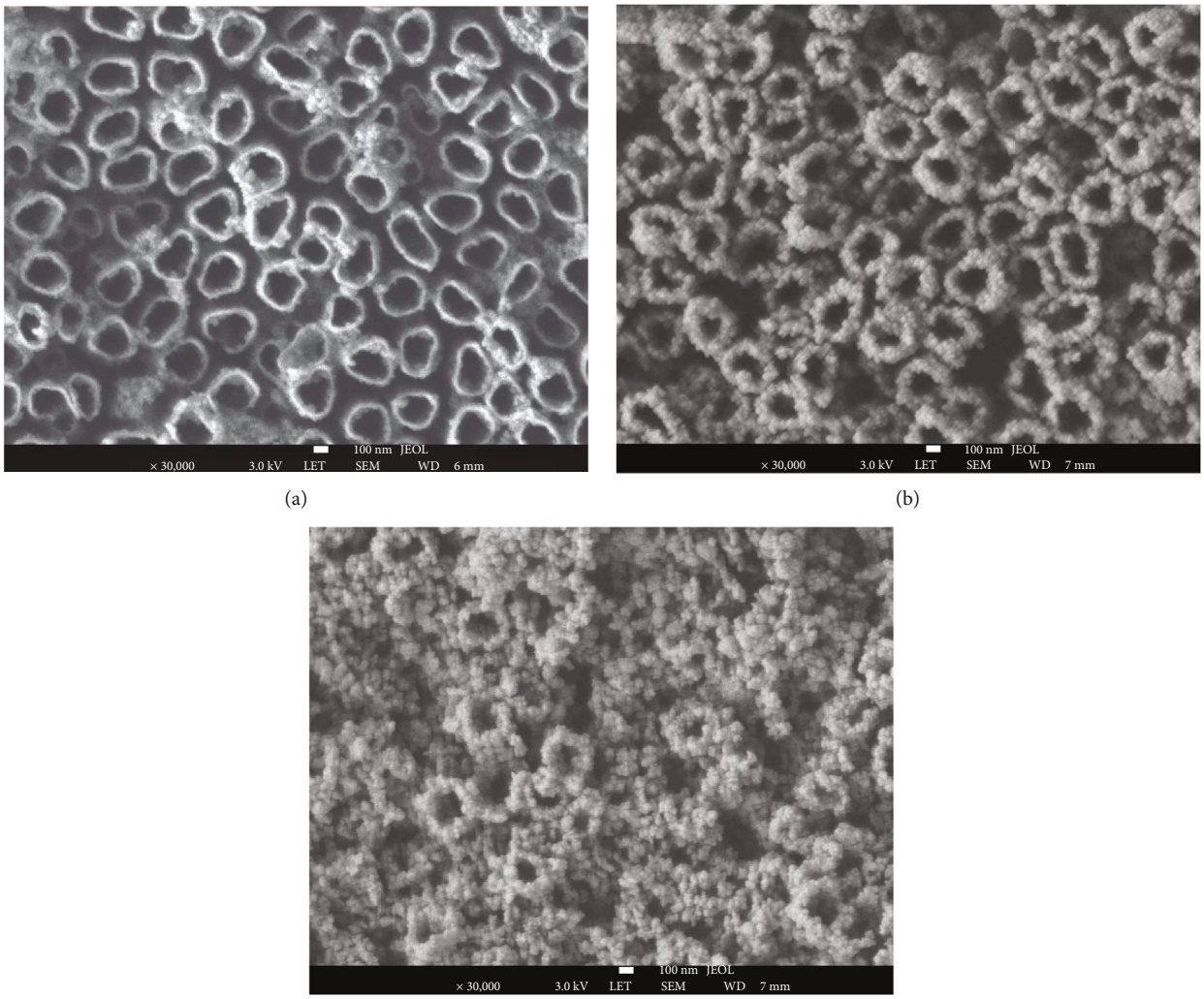

(a) (b)

(c)

Figure 3: The SEM images of LTAs decorated by different concentrations: (a) 7.5×10^{-4} M; (b) 1.2×10^{-3} M; (c) 1.6×10^{-3} M.

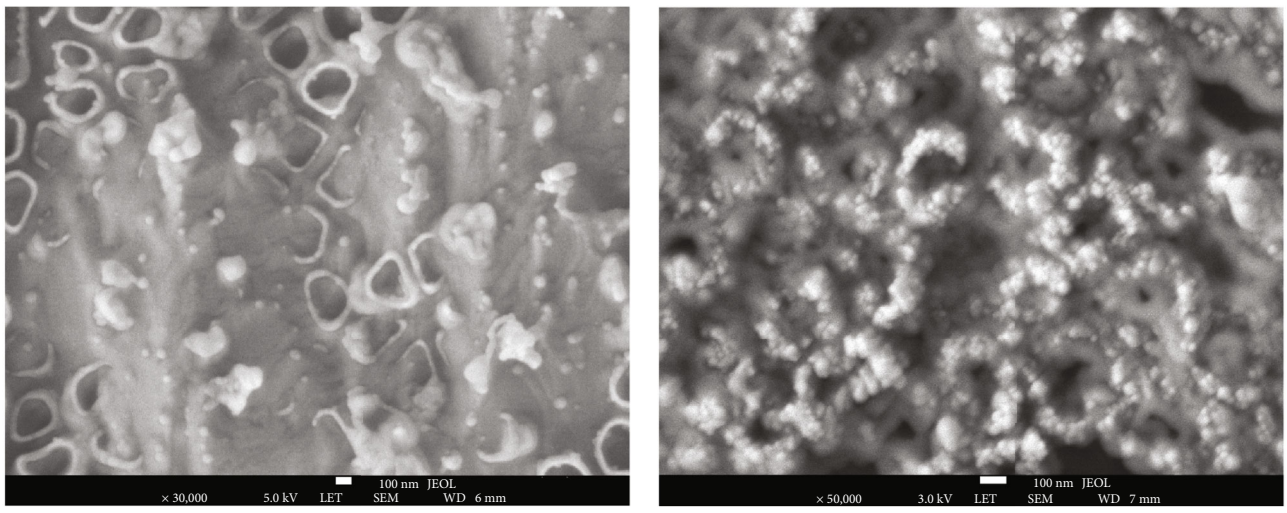

(a) (b)

Figure 4: SEM images of two samples: (a) LTAs after drug loading; (b) TNTs-P25 after drug loading.

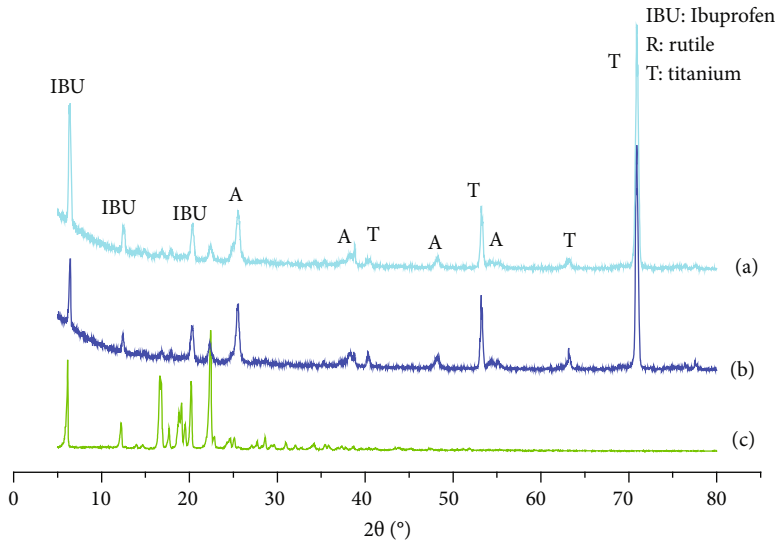

Figure 5: XRD pattern of the samples: (a) LTAs-P25 after drug loading; (b) LTAs after drug loading; (c) pure IBU.

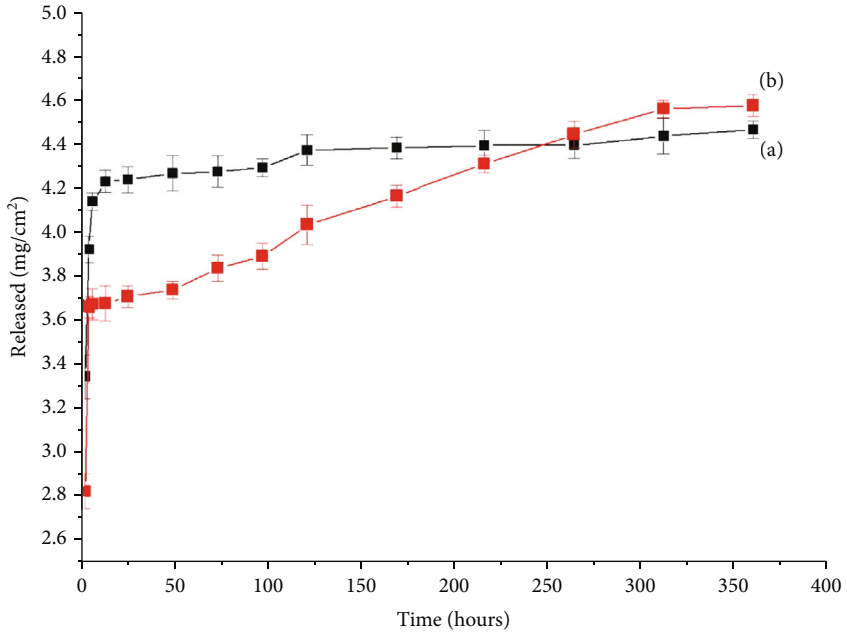

Figure 6: Drug released profiles from (a) LTAs loaded with IBU; (b) TNTs-P25 loaded with IBU.

and the drug release phase of LTAs-P25 consist of the initial 5 h drug burst release and the subsequent 15-day slow-release process. During the 5 h burst release period, the released drugs mainly came from covering the surface and the nozzle, and these drug molecules will diffuse into PBS very quickly. At this stage, the amount of IBU released was about 92.7%. However, the IBU released by LTAs-P25 decreased to 80.2% in the same time period. Subsequent sustained release for up to 15 days mainly comes from IBU loaded on the tube wall and inside the nanotubes. It was concluded that LTAs-P25 provided a lower burst and longer release time. A comparison with the literature [13] showed that the total amount of drug released from LTAs increased by 49.5% compared to that from TiO_2 nanotube arrays without large clearance (from 2.99 mg cm^{-2} to 4.47 mg cm^{-2}). Although the specific surface area and roughness of the LTAs significantly increased, which was conducive to improving the load effect of IBU, the released amount of IBU did not significantly increase for LTAs-P25 in the release stage due to its large void spaces.

4. Conclusions

In this paper, P25 NPs were successfully decorated on the surface of LTAs via hydrothermal treatment under the

optimal conditions, with the pore diameter decreasing to 100 ± 10 nm after decoration. The specific surface area and roughness of the nanotubes were increased after the P25 nanoparticles are loaded on LTAs by a hydrothermal method. The optimum concentration for loading P25 in LTAs more uniformly is 1.2×10^{-3} M. The increased specific surface area and roughness of LTAs after hydrothermal treatment are conducive to drug dispersion and absorption, which was beneficial to improve the load degree and quantity of IBU. The total amount of drug released from LTAs increased by 49.5% compared to that from TiO_2 nanotube arrays without large clearance. Notably, the increase in roughness and surface area of LTAs gave rise to the sustained release of drugs. This is indispensable for the implantation of biomedical materials, especially plastic surgery. These results demonstrate the fact that LTAs-P25 has potential application value in constructing drug delivery systems applied in the biomedical field.

Data Availability

No data were used to support this study.

Conflicts of Interest

The authors declare that they have no conflicts of interest.

Authors' Contributions

Tao Zhang and Nannan Liu contributed equally to this work.

Acknowledgments

This work was financially supported by the Project of innovation platform for Fuzhou Health and Family Planning Commission (Nos. 2018-S-wp3 and 2020-S-wp2), the Key Clinical Specialty Discipline Construction Program of Fujian Province, the Major Science and Technology Projects of Fuzhou (2017), the Funds for young and middle-aged experts with outstanding contributions to health and family planning in Fujian Province (2017-2018), the Project of Fuzhou Science and Technology (No. 2019-SZ-14), the Fifth Round Health Education Joint Project of Fujian Province (No. 2019-WJ-22), and the Natural Science Foundation of Fujian Province (No. 2020J011194).

References

[1] A. de Stefani, G. Bruno, G. Preo, and A. Gracco, "Application of nanotechnology in orthodontic materials: a state-of-the-art review," *Dentistry Journal*, vol. 8, no. 4, p. 126, 2020.

[2] T. Saydé, O. el Hamoui, B. Alies, K. Gaudin, G. Lespes, and S. Battu, "Biomaterials for three-dimensional cell culture: from applications in oncology to nanotechnology," *Nanomaterials*, vol. 11, no. 2, p. 481, 2021.

[3] A. J. Clasky, J. D. Watchorn, P. Z. Chen, and F. X. Gu, "From prevention to diagnosis and treatment: biomedical applications of metal nanoparticle-hydrogel composites," *Acta Biomaterialia*, vol. 122, pp. 1–25, 2021.

[4] C. Karaman, O. Karaman, N. Atar, and M. L. Yola, "Electrochemical immunosensor development based on core-shell high-crystalline graphitic carbon nitride@carbon dots and $Cd_{0.5}Zn_{0.5}S$/d-$Ti_3C_2T_x$ MXene composite for heart-type fatty acid–binding protein detection," *Microchimica Acta*, vol. 188, no. 6, p. 182, 2021.

[5] H. Karimi-Maleh, M. L. Yola, N. Atar et al., "A novel detection method for organophosphorus insecticide fenamiphos: molecularly imprinted electrochemical sensor based on core-shell Co_3O_4@MOF-74 nanocomposite," *Journal of Colloid and Interface Science*, vol. 592, no. 185, pp. 174–185, 2021.

[6] C. Karaman, "Orange peel derived-nitrogen and sulfur co-doped carbon dots: a nano-booster for enhancing ORR electrocatalytic performance of 3D graphene networks," *Electroanalysis*, vol. 33, no. 5, pp. 1356–1369, 2021.

[7] S. Jafari, B. Mahyad, H. Hashemzadeh, S. Janfaza, T. Gholikhani, and L. Tayebi, "Biomedical applications of $_{TiO2}$ nanostructures: recent Advances," *International Journal of Nanomedicine*, vol. 15, pp. 3447–3470, 2020.

[8] D. Kowalski, D. Kim, and P. Schmuki, "TiO_2 nanotubes, nanochannels and mesosponge: Self- organized formation and applications," *Nano today*, vol. 8, no. 3, pp. 235–264, 2013.

[9] K. F. Huo, X. Zhang, H. Wang, L. Z. Zhao, X. Y. Liu, and P. K. Chu, "Osteogenic activity and antibacterial effects on titanium surfaces modified with Zn-incorporated nanotube arrays," *Biomaterials*, vol. 34, no. 13, pp. 3467–3478, 2013.

[10] Y. Hu, K. Cai, Z. Luo et al., "TiO_2 nanotubes as drug nanoreservoirs for the regulation of mobility and differentiation of mesenchymal stem cells," *Acta Biomaterialia*, vol. 8, no. 1, pp. 439–448, 2012.

[11] M. Hasanzadeh Kafshgari and W. H. Goldmann, "Insights into theranostic properties of titanium dioxide for nanomedicine," *Nano-Micro Letters*, vol. 12, no. 1, p. 22, 2020.

[12] C. Yao and T. J. Webster, "Prolonged antibiotic delivery from anodized nanotubular titanium using a co-precipitation drug loading method," *Journal of Biomedical Materials Research. Part B, Applied Biomaterials*, vol. 91B, no. 2, pp. 587–595, 2009.

[13] Z. Wang, C. Xie, F. Luo, P. Li, and X. Xiao, "P25 nanoparticles decorated on titania nanotubes arrays as effective drug delivery system for ibuprofen," *Applied Surface Science*, vol. 324, pp. 621–626, 2015.

[14] G. Devanand Venkatasubbu, S. Ramasamy, V. Ramakrishnan, and J. Kumar, "Folate targeted PEGylated titanium dioxide nanoparticles as a nanocarrier for targeted paclitaxel drug delivery," *Advanced Powder Technology*, vol. 24, no. 6, pp. 947–954, 2013.

[15] Y. Kubota, T. Shuin, C. Kawasaki et al., "Photokilling of T-24 human bladder cancer cells with titanium dioxide," *British Journal of Cancer*, vol. 70, no. 6, pp. 1107–1111, 1994.

[16] A. Hu, L. Xiao, G. Dai, and Z. Xia, "P25 niblet-like coated on large void space TiO_2 nanotubes arrays for high-rate charge-collection and improved photoconversion efficiency," *Journal of Solid State Chemistry*, vol. 190, pp. 130–134, 2012.

[17] Y. Y. Song and P. Schmuki, "Modulated TiO_2 nanotube stacks and their use in interference sensors," *Electrochemistry Communications*, vol. 12, no. 4, pp. 579–582, 2010.

[18] X. F. Xiao, K. G. Ouyang, R. F. Liu, and J. H. Liang, "Anatase type titania nanotube arrays direct fabricated by anodization without annealing," *Applied Surface Science*, vol. 255, no. 6, pp. 3659–3663, 2009.

[19] L. Liu, J. S. Qian, B. Li et al., "Fabrication of rutile TiO_2 tapered nanotubes with rectangular cross-sections via anisotropic corrosion route," *Chemical Communications*, vol. 46, no. 14, pp. 2402–2404, 2010, 14.

[20] A. Z. Hu, L. X. Xiao, G. P. Dai, and Z. C. Xia, "P25 niblet-like coated on large void space TiO_2 nanotubes arrays for high-rate charge-collection and improved photoconversion efficiency," *Advanced Powder Technology*, vol. 24, pp. 947–954, 2013.